A STUDY OF A POROUS COMBUSTOR WITH A BUILT-IN HEAT EXCHANGER

Roberto Carlos Moro Filho, moro@ect.ufrn. br
Amilcar Porto Pimenta, amilcar@ita.br
Escola de Ciências e Tecnologia-ECT
Universidade Federal do Rio Grande do Norte – UFRN
59072-970 – *Natal – RN - Brasil*

Abstract. Premixed combustion inside a porous medium is currently under investigation due to the characteristics of this technology which provides controlled flames. The present work presents numerical methods for the simulation of premixed methane/air flames in porous media using a six step reduced mechanism. The laminar two dimensional model is based on a macroscopic formulation of the heat and mass transport equations for laminar flow. Finite volume method is used for simulation with a boundary-fitted non-orthogonal coordinate system. The effects of the model on temperature and species are examined in a porous burner. The results are compared with the experiment available in the literature. The CO mass fraction calculated is compared with the available experimental data. The good agreement with the experimental data suggests that the numerical model is an excellent tool to investigate pollutants formation.

Keywords: porous media burner, premixed flame, numerical simulation.

1. INTRODUCTION

The necessity of improvements in the gas-burner technology focusing efficiency and reduction of emission of pollutants has led to the development of new burner concepts. Premixed combustion inside a porous medium is currently under investigation due to the characteristics of this technology which provides controlled flames. Burning of lean combustible mixtures, higher ranges of flame stability and lower pollutant formation are some of the advantages of this technology. Systems based on fluidized bed combustion, in-situ combustion for oil recovery, household heating combustion, are just a few examples of such applications (Howell *et al.* (1996); Trimis and Durst (1996)).

In most of the studies of premixed combustion within inert porous media the flow is assumed to be laminar and one-dimensional, the variation in the pressure across the flame is generally negligible compared with the absolute pressure, and the pressure is assumed constant (Baek (1989); Yoshizawa *et al.* (1988); Hsu *et al.* (1993); Neef *et al.* (1999)). The use of single-step global chemistry (Mohamad *et al.* (1994); Sathe *et al.* (1990)) is common, but, the inadequacies of global kinetics are well recognized. Hsu *et al.* (1993) presents a comparison between one-step and multi-step chemistry.

Studies on macroscopic transport modeling of incompressible flows in porous media have been based on the volume-average methodology for either heat or mass transfer (Kaviany (1995)). Because of important influence of lateral heat loss in porous medium burners, a two dimensional model is necessary (Brenner *et al.* (2000)).

The present paper follows the foregoing works and presents a two dimensional mathematical model for laminar premixed flame combustion in porous media. The numerical methodology employed is based on the control-volume approach with a boundary-fitted non-orthogonal coordinate system. In order to achieve steady combustion in the porous media the reactor has a steep gradient in the pore size of the porous matrix. The reactor studied in this work has three-region burner with a small pore size in the first region and a large pore size downstream in the second and third region. The flame can be stabilized at the interface between the two different porosity blocks. The main goal of this study is to develop a computational code to investigate the choice of materials in each porous region, pre-heating region and combustion region, and the influence of this choice on the pollutants emission. Thermal nonequilibrium was subject of previous work (Moro and Pimenta (2009)). Dispersion and sensitivity analyses with respect to the thermal physical properties are subjects of ongoing investigations and will be addressed in subsequent papers.

2. MACROSCOPIC TRANSPORT EQUATIONS

2.1 Macroscopic continuity equation

$$\phi \left\langle \frac{\partial \rho}{\partial t} \right\rangle^f + \nabla.(\langle \rho \rangle^f \mathbf{u}_D) = 0 \tag{1}$$

where, $\mathbf{u}_D$ is the average surface velocity (also known as seepage, superficial, filter or Darcy velocity). Equation (1) represents the macroscopic continuity equation.

2.2 Macroscopic momentum equation

$$\frac{\partial(\rho\mathbf{u}_D)}{\partial t} + \nabla\cdot\left(\frac{\rho\mathbf{u}_D\mathbf{u}_D}{\phi}\right) = -\nabla(\phi\langle p\rangle^f) + \mu\nabla^2\mathbf{u}_D - \left[\frac{\mu\phi}{K}\mathbf{u}_D + \frac{c_F\phi\rho|\mathbf{u}_D|\mathbf{u}_D}{\sqrt{K}}\right] \tag{2}$$

where the last two terms in equation (2), represent the Darcy-Forchheimer contribution (Pedras (2000)). The symbol K is the porous medium permeability, $c_F = 0.55$ is the form drag coefficient (Forchheimer coefficient), $\langle p\rangle^f$ is the intrinsic (volume-averaged on fluid phase) pressure of the fluid, ρ is the fluid density and is a function of temperature, μ represents the fluid dynamic viscosity and ϕ is the porosity of the porous medium.

2.3 Macroscopic Energy Equation

$$\left\{(\rho c_p)_f\phi + (\rho c_p)_s(1-\phi)\right\}\frac{\partial\langle T\rangle}{\partial t} + (\rho c_p)_f\nabla\cdot(\mathbf{u}_D\langle T\rangle) =$$

$$\nabla\cdot\left\{\mathbf{K}_{eff,f}\cdot\nabla\langle T\rangle\right\} + \phi\left\langle\sum_{k=1}^{Nsp}\overset{\bullet}{w}_k M_k h_k\right\rangle^f \tag{3}$$

where, $\langle T\rangle = \langle T\rangle^f = \langle T\rangle^s$ is the averaged temperature for both the solid and the liquid according to the concept of local thermal equilibrium (Rocamora (2001); Kaviany (1995)), h_k is the specific enthalpy of species k, w_k is the molar rate of reaction of species k, M_k is the molecular weight of species k, $\mathbf{K}_{eff}$ is the effective conductivity tensor given by,

$$\mathbf{K}_{eff} = \left\{\phi k_f + (1-\phi)\left[k_s + \frac{16\sigma(\langle T\rangle)^3}{3K_r}\right]\right\}\mathbf{I} + \underbrace{\mathbf{K}_{tor}}_{tortuosity} + \underbrace{\mathbf{K}_{disp}}_{dispersion} \tag{4}$$

where, k_f and k_s are the thermal conductivities for the fluid and for the solid, K_r is the local Rosseland mean attenuation coefficient, σ is the Stefan-Boltzmann constant, $\mathbf{K}_{tor}$ and $\mathbf{K}_{disp}$ are the tortuosity and thermal dispersion conductivity tensors, respectively.

The radiation in an optically dense medium can be modeled using the diffusion approximation or Rosseland model (Siegel and Howell (2002)). In the radiative diffusion approximation the radiation is computed like an increase in the effective conductivity and is represented by the term containing K_r in equation (4). For a combustion occurring inside a ceramic, with a small solid conductivity like Zirconium Oxide, the conductivity due to radiation can represent more than 80% of the total conductivity, hence, radiation within the porous media cannot be neglected.

In this work the effects of dispersion and tortuosity are neglected, hence, the last two terms on the right in equation (4) are not being considered.

2.4 Macroscopic Mass Transport Equation

$$\frac{\partial(\rho\phi\langle y_k\rangle^f)}{\partial t} + \nabla\cdot(\rho\mathbf{u}_D\langle y_k\rangle^f) = \nabla\cdot[\rho\mathbf{D}_{eff}\cdot\nabla(\phi\langle y_k\rangle^f)] + \phi\left\langle\overset{\bullet}{w}_k M_k\right\rangle^f \tag{5}$$

where y_k is the local mass fraction for the species k. The effective dispersion tensor D_{eff} is defined as:

$$\mathbf{D}_{eff} = \mathbf{D}_{disp} + \mathbf{D}_{diff} = \mathbf{D}_{disp} + \frac{1}{\rho}\left(\frac{\mu}{Sc}\right)\mathbf{I} \tag{6}$$

where, Sc is the Schimidt number, D_{diff} is the macroscopic diffusion tensor, and D_{disp} is the mass dispersion tensor (Mesquita (2003)). The effects of dispersion are neglected in this work, therefore, the effective dispersion tensor is given by:

$$\mathbf{D}_{eff} = \langle D\rangle^f I = \frac{1}{\rho}\left(\frac{\mu}{Sc}\right)\mathbf{I} \tag{7}$$

2.5 Boundary conditions

The following boundary conditions are imposed on the solution:

$$\text{at } x=0, \; u= u_{in}, \; v=0, \; \langle T \rangle = T_{in}, \; \langle y_k \rangle^f = y_{k,in}, \tag{8}$$

$$\text{at } x=L, \; \frac{\partial \langle y_k \rangle^f}{\partial x} = \frac{\partial u}{\partial x} = \frac{\partial v}{\partial x} = 0, \tag{9}$$

$$\text{and } -\frac{\partial \langle T \rangle}{\partial x} = \sigma T_s^{\,4} \tag{10}$$

where, u and v are the components of Darcy velocity vector in x and y. It was considered heat losses at the walls and at the exit. At the exit, it was considered a heat flux by radiation calculated as a black body at the temperature T_s of 673 K. At the wall surfaces the no-slip and impenetrability conditions were applied to the momentum equations and the gradient of mass fraction to the surface was zero. At the outer wall boundaries the temperature was that of the water of the refrigeration to be heated 40°C (See figure 1). These temperatures were considered according to the work of Brenner *et al.* (2000). The heat flux to the cooled surfaces is given by

$$q = -K_{eff} \frac{\partial \langle T \rangle}{\partial n} = \frac{\langle T \rangle - T_c}{R_t} \tag{11}$$

where, R_t is the total thermal resistance and T_c is the temperature of the coolant.

3. COMBUSTION MODEL

The method to solve the chemical kinetic problem utilizes two models to describe the reaction process, a global reaction mechanism is used as a first approximation, following a six step reaction mechanism.

3.1.1 One-step global mechanism

The combustion reaction is assumed to occur in a single step according to the chemical equation

$$CH_4 + 2(1+\Psi)(O_2 + 3.76N_2) \longrightarrow CO_2 + 2H_2O + 2\Psi O_2 + 7.52(1+\Psi)N_2 \tag{12}$$
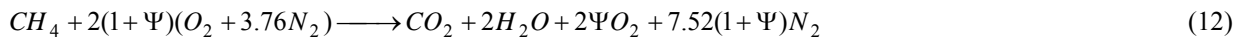
where, ψ is the excess air in the reactant stream at the inlet of porous foam and is related to the equivalence ratio Φ by,

$$\Psi = \frac{1}{\Phi} - 1 \tag{13}$$

where,

$$\Phi = \frac{(y_{fu} / y_{ox})}{(y_{fu} / y_{ox})_{st}} \tag{14}$$

The ratio of fuel consumption is given by,

$$S_{fu} = \rho^2 A \langle y_{fu} \rangle^f \langle y_{Ox} \rangle^f \exp(-E_a / R\langle T \rangle) \tag{15}$$

where, A is the pre-exponential factor, E_a is the activation energy and R is the universal gas constant. The gas density is updated using the ideal gas equation in the form,

$$\rho = P_0 / R^* \langle T \rangle \tag{16}$$

where, P_0 is a reference pressure, which is kept constant during the relaxation process, and $R^* = R / M$ and M is the gas molecular mass.

3.1.2   Six-step reduced mechanism

Chang and Chen have developed a six-step reduced mechanism with an automatic computer code (CARM) from GRI-MECH 1.2:

(I) $2O = O_2$
(II) $H + O = OH$
(III) $H_2 + O = H + OH$
(IV) $O + (1/2) CH_4 = (1/2) H_2 + (1/2) H + (1/2) OH + (1/2) CO$
(V) $O + CO = CO_2$
(VI) $O + H_2O + (1/4) CO = (1/4) H_2 + (1/4) H + O_2 + (1/4) OH + (1/4) CH_4$

4. NUMERICAL MODEL

The governing equations were discretized using the finite volume procedure (Patankar (1980)) with a boundary-fitted non-orthogonal coordinate system. The system of algebraic equations was solved through the semi-implicit procedure according to Stone (1968). The SIMPLE algorithm for the pressure-velocity coupling was adopted to correct both the pressure and the velocity fields. The process starts with the solution of the two momentum equations. Then the velocity field is adjusted in order to satisfy the continuity principle. This adjustment is obtained by solving the pressure correction equation. The energy and species equations are solved using a fractional time step method (Yanenko (1971)) to eliminate the problems arising from the stiffness of the system. It was adopted the minimum residence time of the gas in all control volumes as the integration time step. Calculations start using one-step global kinetics mechanism, when the residuals reach 1×10^{-3} the multistep mechanism is switched on and the fractional time step method is applied (Malico et $al.$ (2000)). The kinetic problem is solved using the Chemkin 4.1 (Kee et $al.$ (2004)) with a six step mechanism. A computational mesh of 402x24 nodes is used in x- and y-direction in the simulations. All computations were performed on an AMD Athlon™ X2 5000 with double precision. For all cases a relative convergence of 10^{-5} was specified. The grid effects on the solutions were examined by increasing the number of nodes and verifying the solutions until the results no longer changed in a specified tolerance. The average computational time was 12 hours.

5. RESULTS AND DISCUSSION

A rectangular 10 kW porous burner prototype developed and tested at LSTM-University of Erlangen-Nuremberg (Brenner et $al.$ (2000)) was considered in this study. Figure 1 presents the geometry of the porous media burner consisting of two distinct regions, a preheating region with small pores is followed by the combustion region with large pores size. The preheating region was composed of zirconium oxide foam with 18 pores per linear centimeter (ppcm). This region was surrounded by heat conducting aluminium bars to remove heat and prevent flashback. The gas mixture enters at the inflow boundary on the left, and the combustion products leave the burner at the outflow boundary on the right.
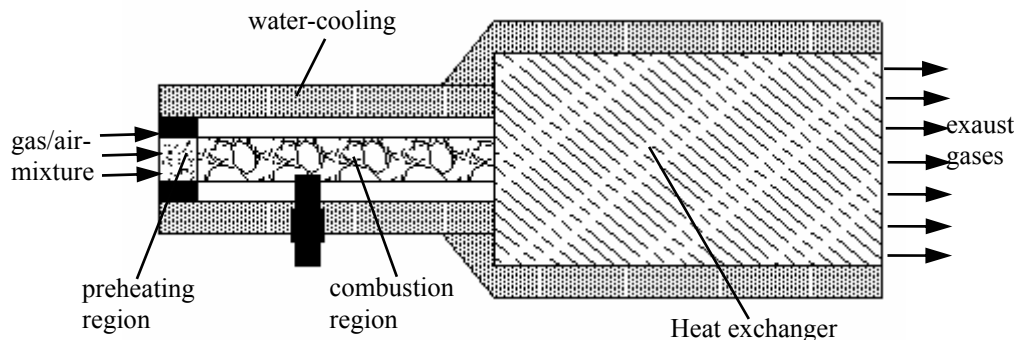

Figure 1. Geometry of a rectangular porous burner according to Brenner et $al.$ (2000).

The combustion region (Figure 2) consists of two porous matrix, the first one (combustion region (A)) is a zirconium oxide foam with 8 ppcm, and in the following matrix (combustion region (B)) a static mixer-like alumina fiber with a lamellae height of 8mm, a lamellae wave length of 20 mm, and a lamellae angle of 45º. The combustion chamber walls were insulated with a 10 mm layer of alumina fiber material. The walls of the burner are water cooled, the preheating region has a large heat flux at the walls through the aluminium bars, the combustion region is insulated

with a ceramic material in order to avoid incomplete reactions. Table 1 presents the parameters adopted in the simulations.
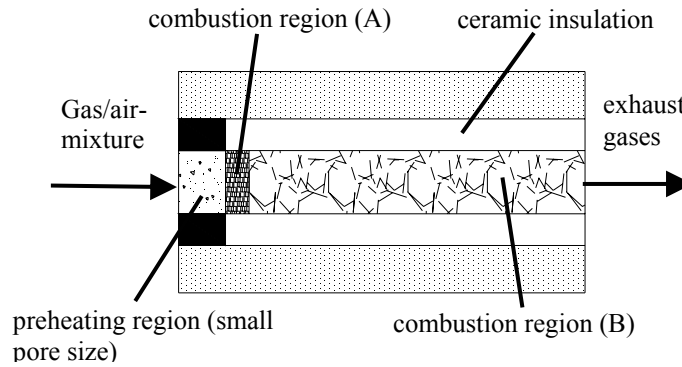

Figure 2. Schematic diagram of the preheating region and the combustion region.

Figure 3 presents the pressure drop at the center line of the combustor where,

$$PN = \frac{P - P_{MIN}}{P_{MAX} - P_{MIN}} \tag{17}$$

there are inflection points at the abscissas x/L=0.15 and x/L=0.23 approximately, representing the interfaces between the porous materials. It was observed with additional simulations that the combustion affects the pressure drop slightly when compared with the flow without combustion in this kind of combustor.
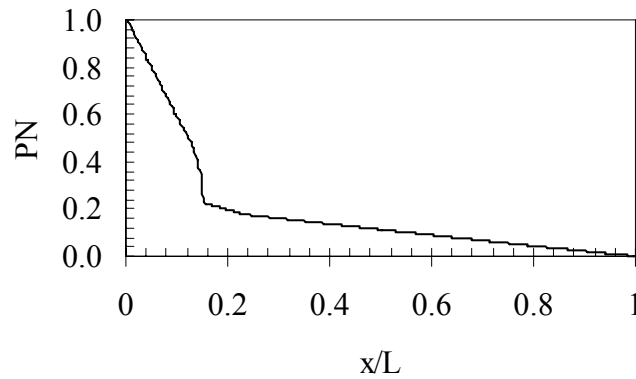

Figure 3. Pressure drop at the center line of the combustor.

The thermal physical properties of the fluid were obtained from the Chemkin 4.1 thermodynamic property database (Kee *et al.* (2002)), the solid properties were taken from the polynomials of Brenner *et al.* (2000) and they provided that the variations with temperature were considered. The predicted temperature field in figure 4 was obtained considering the heat removal at the exit by radiation of a black body with a temperature of 673 K, the heat removal at the walls boundary was obtained considering that the outer water of the refrigeration heated 40ºC. The stabilization process was obtained without artifice, after the ignition, combustion is self-stabilized just solving the set of equations with a first approximation provided by the same case simulated using the global mechanism.
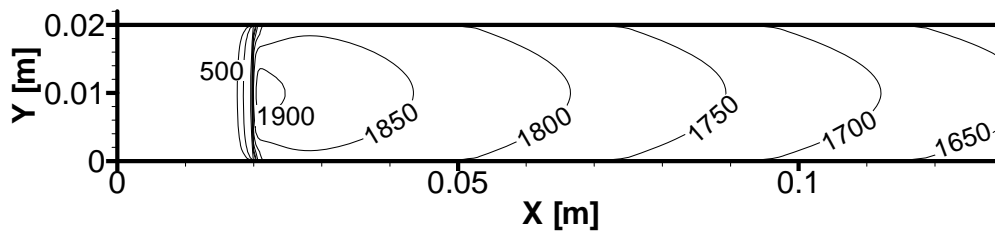
Figure 4. Field of predicted temperature (K) for a 2650 kW/m2 power, and equivalence ratio of 0.77.

In figure 5 is presented the CO mass fraction at the center line of the reactor, a comparison between experimental and numerical results. The difference between numerical solutions and experiment can be attributed to the uncertainness about some parameters such as solid conductivity, solid heat capacity, and Rosseland mean attenuation coefficient. The uncertainness about the water cooler system and the heat flux at the wall is another point that needs to be reviewed.
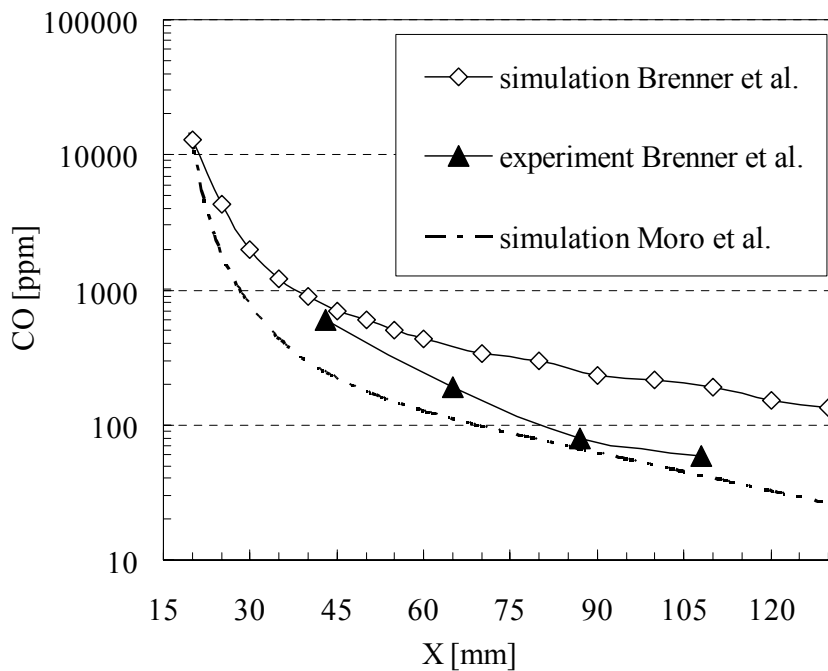

Figure 5. Comparison of calculated and measured CO data.

It is presented in figure 6 the fields of some species obtained with a 6 step mechanism in a 2650 kW/m^2 power and equivalence ratio of 0.77. The preheating region has a small pore size, smaller than the quench distance to prevent flashback. The flame stabilizes at the combustion region due to the energy balance and the basic principle where the velocity of the flow is equal to the flame velocity in a stabilized flame. The operating parameters are presented in table 1.
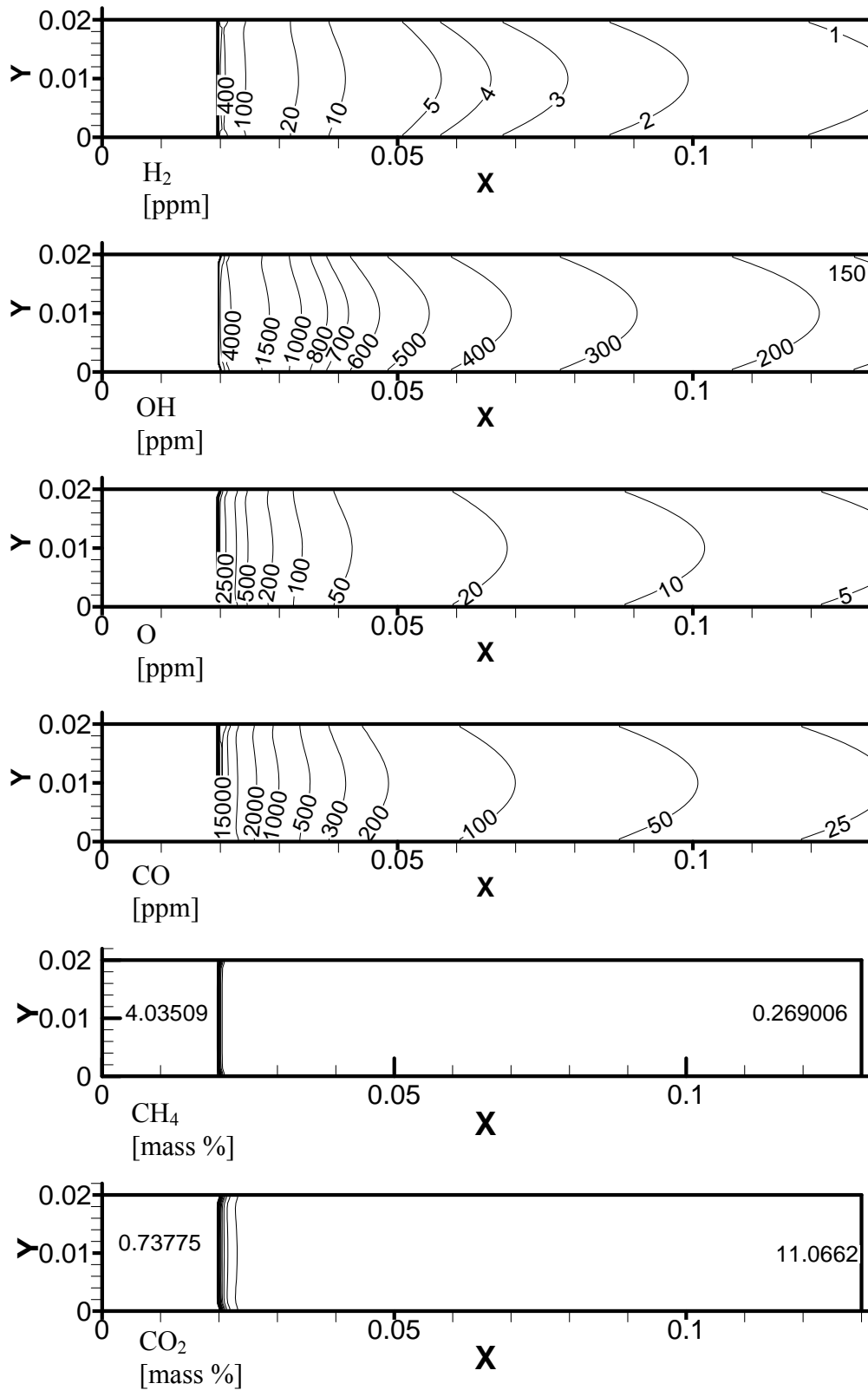
Figure 6. Fields of calculated mass fraction for 2650 kW/m2, and equivalence ratio of 0.77.

Table 1. Operating Conditions Burner I

Quantity	Value
Length of the combustor chamber $-$ L(cm)	13
H (cm)	2
yfuel,in	0.04304086
Firing rate (kW)	10
Inlet gas temperature (K)	300
Equivalence ratio	0.77
Porosity1	0.5
Porosity2	0.8
Porosity3	0.95
P_0 (kN/m2)	101.325
E_a	140×10^3 J/mol
A	1×10^{10} m^{3}kg^{-1}s^{-1}

6. Conclusion

A mathematical model has been developed, and numerically obtained results compared with available experimental data for a porous burner. Temperature, mass fraction of some species, flame location, and pressure drop have been predicted. Numerical results compared reasonably well with the experimental data, in spite of the high uncertainty about the thermal physical parameters.

The model can be used to predict the fields of temperature, mass fraction of the species, pressure drop, and velocity. There are a lot of properties of the composites that need to be more investigated experimentally. There is a high uncertainness about porosities, thermal physical properties, radiative properties, etc. The variations of these properties affect the flame stabilization position and all the variables fields.

7. Acknowledgements

8. REFERENCES

Baek, S. W., 1989, "The Premixed Flame in a Radiatively Active Porous Medium," Combust. Sci. Technol., 64, pp. 277–287.

Brenner, G., Pickenacker, K., Pickenacker, O., Trimis, D., Wawrzinek, K., and Weber, T., 2000, Numerical and Experimental Investigation of Matrix-Stabilized Methane/Air Combustion in Porous Inert Media, Combustion and Flame, 123, pp. 201-213.

Chang ,W.C. , Chen, J.Y., http: http://firebrand.me.berkeley.edu/griredu.html

Howell, J. R., Hall, M. J., and Ellzey, J. L., 1996, "Combustion of Hydrocarbon Fuels Within Porous Inert Media," Prog. Energy Combust. Sci., 22, pp. 121–145.

Hsu, P.-F., Howell, J. R., and Matthews, R. D., 1993, "A Numerical Investigation of Premixed Combustion Within Porous Inert Media," ASME J. of Heat Transfer, 115, pp. 744–750.

Kaviany. M.. 1995. Principles of Heat Transfer in Porous Media. 2nd edn. Springer. New York.

Kee, R. J., F. M. Rupley, J. A. Miller, M. E. Coltrin, J. F. Grcar, E. Meeks,H. K. Moffat, A. E. Lutz, G. Dixon-Lewis, M. D. Smooke, J. Warnatz, G. H. Evans,R. S. Larson, R. E. Mitchell, L. R. Petzold, W. C. Reynolds, M. Caracotsios, W. E. Stewart, P. Glarborg, C. Wang, C. L. McLellan, O. Adigun, W. G. Houf, C. P. Chou, S. F. Miller, P. Ho, P. Young, D. J. Young, CHEMKIN Release 4.0, Reaction Design, San Diego, CA (2004).

Malico, I., Zhou, X.Y., and Pereira, J.C.F., 2000, Two-dimensional Numerical Study of Combustion and Polutants Formation in Porous Burners, Com,bust. Sci. and Tech., 152, pp. 57-79.

Mesquita, M.S., 2003, Análise da dispersão mássica em meios porosos em regimes laminar e turbulento. Tese de doutorado, Instituto Tecnológico de Aeronautica, Brasil.

Mohamad, A.A., Ramadhyani, S., Viskanta, R, 1994.Modeling of Combustion and Heat-Transfer in a Pcked-Bed with Embedded Coolant Tubes, Int. J Heat and Mass Transfer. vol. 37. (8) pp.1181-1191.

Moro Filho, R. C.; Pimenta, Amilcar . A numerical study of combustion in porous burner with a two-energy equation model, Gramado-RS, 20th International Congress of Mechanical Engineering, 2009.

Neef, M., Knaber, P., Summ, G., 1999, Numerical Bifurcation Analysis of Premixed Combustion in Porous Inert Media, unpublished, http://citeseer.csail.mit.edu/197085.html

Patankar. S. V.,1980. Numerical Heat Transfer and Fluid Flow. Hemisphere. New York.

Pedras, M.H.J., 2000, Análise do Escoamento Turbulento em Meio Poroso Descontínuo. Tese de doutorado, Instituto Tecnológico de Aeronautica, Brasil.

Rocamora, F.D.J., 2001, Análise do transporte de calor em regime laminar e turbulento em meio poroso descontínuo. Tese de doutorado, Instituto Tecnológico de Aeronautica, Brasil.

Sathe, S.B., Peck, R.E., and Tong, T.W., 1990, Flame Stabilization and Multimode Heat Transfer in Inert Porous Media: A Numerical Study, Combust. Sci. and Tech., Vol. 70, pp. 93-109.

Siegel, Robert, and, Howell, John, 2002, Thermal Radiation Heat Transfer, 4th edition.

Stone, H. L., SIAM J. Num. Anal. 5:530-558 (1968).

Thermodynamic data is part of the CHEMKIN Collection. R. J. Kee, F. M. Rupley, J. A. Miller, M. E. Coltrin, J. F. Grcar, E. Meeks, H. K. Moffat, A. E. Lutz, G. Dixon-Lewis, M. D. Smooke, J. Warnatz, G. H. Evans, R. S. Larson, R. E. Mitchell, L. R. Petzold, W. C. Reynolds, M. Caracotsios, W. E. Stewart, P. Glarborg, C. Wang, O. Adigun, W. G. Houf, C. P. Chou, and S. F. Miller, Chemkin Collection, Release 3.7, Reaction Design, Inc., San Diego, CA (2002).

Trimis, D., and, Durst, F., 1996, Combustion in a Porous Medium Advances and Applications, Combust. Sci. Technol, Vol. 121, pp. 153-168.

Yanenko, N. N. (l97l). The method of fractional time steps: the solution of problems of mathematical phisics in several variables, M . Holt (Editor), Springer-Verlag, New York.

Yoshizawa, Y., Sasaki, K., and Echigo, R., 1988, "Analytical Study of the Structure of Radiation Controlled Flame," Int. J. Heat Mass Transf., 31, pp. 311–319. [Inspec] [ISI]